IEEE Access
Multidisciplinary | Rapid Review | Open Access Journal

Received July 9, 2017, accepted August 14, 2017, date of publication August 23, 2017, date of current version October 12, 2017.

Digital Object Identifier 10.1109/ACCESS.2017.2742142

Energy Control Strategy of HEB Based on the Instantaneous Optimization Algorithm

DAPAI SHI[1], LIANG CHU[1], (Member, IEEE), JIANHUA GUO[1], GUANGDONG TIAN[2], YIXIONG FENG[3], AND ZHIWU LI[4,5], (Fellow, IEEE)

[1]State Key Laboratory of Automotive Dynamic Simulation and Control, Jilin University, Changchun 130022, China
[2]Transportation College, Jilin University, Changchun 130022, China
[3]State Key Laboratory of Fluid Power Transmission and Control, Zhejiang University, Hangzhou 310027, China
[4]Institute of Systems Engineering, Macau University of Science and Technology, Macau 999078, China
[5]School of Electro-Mechanical Engineering, Xidian University, Xian 710071, China

Corresponding authors: Jianhua Guo (gjhjlu@163.com), Guangdong Tian (tiangd2013@163.com), and Yixiong Feng (fyxtv@zju.edu.cn)

This work was supported in part by the Jilin Science and Technology Development Plan Project under Grant 20170204085GX, in part by the 863 National High Technology Research and Development Program of China under Grant 2012AA110903, in part by the National Natural Science Foundation of China under Grant 51405075 and Grant 51775238, and in part by the Jilin Industrial Technology Innovation Strategic Alliance Project under Grant 20150309013GX.

ABSTRACT In order to solve the problems of high gas consumption and low battery power in hybrid electric buses, the logic threshold control strategy is optimized by the key technology research of driving conditions, control strategy, and so on. First, driving condition data of hybrid electric buses are collected and analyzed, and three typical working conditions are selected. Second, the torque distribution control strategy is investigated based on the instantaneous optimization algorithm. The objective function of the instantaneous equivalent fuel consumption is derived. The process of solving the objective function is attributed to linear programming problem of the nonlinear objective function. The SIMULINK model of instantaneous torque distribution strategy is established based on equivalent fuel consumption. On this basis, the SIMULINK model of the function which can be integrated into the vehicle control model is established. Then, considering the actual driving conditions of the bus, the vehicle control strategy model is established in the MATLAB/SIMULINK environment, and the vehicle model established by the cruise software. Finally, the vehicle model is simulated under three representative working conditions. The main contribution of this paper is the optimized torque distribution control strategy to control hybrid electric bus's energy distribution and reduce emissions. The strategy can be obtained by combining the logic threshold torque distribution control strategy, along with the optimal engine torque and motor torque, which can be obtained by solving the objective function of instantaneous equivalent fuel consumption. Results show that compared with the logic threshold value torque distribution control strategy, the energy control strategy of the instantaneous optimization algorithm can further reduce gas consumption and maintain the state of charge value balance of the power battery.

INDEX TERMS Parallel hybrid electric bus, driving condition, logic threshold value, instantaneous optimization, torque distribution control strategy.

NOMENCLATURE

b_e	Instantaneous fuel consumption rate of the engine.
b_{e_req}	Instantaneous required fuel consumption rate of the engine.
$\overline{b}_{chg}$	Average instantaneous fuel consumption rate of the engine when charging the battery.
$\overline{b}_{chg}$	Average fuel consumption rate of the battery charge in the n control period of the future under the current discharge condition.
b_{mc_chg}	Fuel consumption rate of the battery charging at current time of battery charging condition.
$\overline{b}_{cyc\_chg}$	The average fuel consumption rate.
ΔC	Battery capacity at the current control cycle.
ΔC_{ess_rep}	Future compensation power of the battery.
ΔC_{ess_chg}	Power battery capacity when charging the battery.
DEV_{SOC}	SOC value which deviates from the optimum value.

G_r	Required amount of fuel.
I	Battery output current.
$J_{\min}$	Objective function of the instantaneous equivalent fuel consumption.
k	Number of shift.
K_{soc}	Penalty coefficient of SOC.
m_{rep}	Instantaneous fuel consumption of the motor.
$\dot{m}_{fc}$	Instantaneous fuel consumption function of the engine.
$\dot{m}_{mc\_eq}$	Instantaneous equivalent fuel consumption functions of the motor.
$\dot{m}_{mc\_eq}$	Instantaneous fuel consumption equivalent function of the motor.
$M_{\text{mode\_1}}$	Action time segments in the joint drive.
$M_{\text{mode\_6}}$	Action time segments in the sliding charge.
$M_{\text{mode\_7}}$	Action time segments in the brake energy operation mode.
P_{drv}	Driving power.
P_{fc}	Engine output power.
P_{mc}	Assisted motor power.
P_{mc_rep}	Power of motor power generation.
P_{mc_chg}	Motor power when charging battery.
P_{mc_rep}	Power of the motor power generation.
P_{ess}	Battery output power.
$P_{motorbrake}$	Amendment power of the battery energy consumption under the regenerative braking mode.
$P_{motorcoast}$	Amendment power of the battery energy consumption in the sliding mode.
ρ	Ratio of motor speed to transmission input shaft.
R	Transmission ratio of the main gear reducer and transmission gear box.
SOC_{lo}	Lower limit value of the SOC.
SOC_0	Best value of the SOC value.
$SOC_{initial}$	Initial SOC value of power battery.
SOC_{hi}	Upper limit value of the SOC value.
SOC_{final}	Final SOC value of the power battery.
U_{OC}	Battery voltage.
ΔSOC	Discharge capacity of the battery within a certain period of time.
t	Runtime.
Δt	A certain period of time.
T_{fc}	Instantaneous torque function of the engine.
$T_{fc\_\min}$	Minimum torque value of the engine.
$T_{fc\_\max}$	Maximum torque value of the engine.
T_{mc}	Instantaneous torque function of the motor.
T_{wh}	Instantaneous torque function of the wheel.
ω_{fc}	Instantaneous speed function of the engine.
$\omega_{fc\_\max}$	Maximum speed value of the engine.
$\omega_{fc\_\min}$	Minimum speed value of the engine.
ω_{wh}	Instantaneous speed function of the wheel.
ω_{mc}	Instantaneous speed function of the motor.
η_{gb}	Gear-box efficiency.
η_e	Work efficiency of the engine.
η_{mc}	Working efficiency of the motor.
η_{chg}	Battery charging efficiency.
η_{dis}	Battery discharge efficiency.
$\overline{\eta}_{mc}$	Average efficiency of the motor in the N control period.
$\overline{\eta}_{chg}$	Average charge efficiency of the battery in the N control period.
$\overline{\eta}_{chg}$	Average battery charging efficiency.
$\overline{\eta}_{dis}$	Average battery discharging efficiency.

I. INTRODUCTION

With the aggravation of global warming, shortage of natural resources and environmental pollution, the promotion of hybrid electric bus (HEB) has become one of the effective measures to reduce the energy consumption, relieve the urban traffic pressure, and improve the urban environment [1]–[3]. In many cities in China, such as Hangzhou and Beijing, hybrid buses are already on trial run, but their fuel efficiency rates are not ideal from the actual operating conditions [4]. Due to the irrationality of energy management strategies, some hybrid electric vehicles have a designed fuel saving rate of 30%, but it can only reach 10% or even less in actual operations [5].

Because of its good real-time and easy popularization, logic threshold control strategy is used to control vehicles. The formulation of logical rules is usually based on work characteristic diagrams or expert experience of some components [6], [7]. However, due to the restriction of some objective constraints, the logic based energy management strategy is not optimal for long time complex vehicle operations. Besides, the traditional control strategy does not consider actual driving conditions affected by some dynamic factors [8]. It can only ensure engine working in high efficiency, but does not consider energy loss of the motor or energy conversion. Through the investigation of the actual vehicle running status, it is found that the gas consumption of the HEB is not up to the ideal standard, and the battery state of charge (SOC) is in a low state. In the mean time, the maintenance of SOC is not well [9], [10]. SOC is also called residual power and represents the ratio of the remaining capacity of a battery over a period of time or a long period of time to the capacity on a fully charged state [11], [12]. So the control strategy cannot reach the best efficiency of the whole powertrain [13]–[15]. Because the optimization ability of the logical rule control strategy is limited, the research focus is shifted to energy control strategy based on optimization algorithm and actual driving cycles [16], [17].

In this paper, the instantaneous optimization algorithm is used to design the HEB energy control strategy. The instantaneous optimization control strategy can consider the equivalent fuel consumption of the engine and battery consumption [18], [19]. According to the current speed and demand torque, the reasonable distribution of the engine torque and motor torque can make the equivalent fuel of engine fuel consumption and the consumption of battery power reach the minimum instantaneous value. The control

strategy can also consider the vehicle economy and limitations of emissions by setting up a set of weight coefficients [20].

Through the analysis of bus driving cycles, three representative working conditions are selected and the instantaneous optimal control strategy is used. According to modeling principles and actual driving conditions, the vehicle control strategy is designed on the Matlab/Simulink platform. The vehicle model is established and simulated by cruise software [21]. Under the premise of keeping the power, the goal is to improve the economic performance of the vehicle, further reduce the gas consumption, maintain the balance of battery power and develop an exclusive control strategy which is suitable for the HEB route [22].

In comparison with the existing studies, this work makes three distinctive contributions:

(1) The objective function of instantaneous equivalent fuel consumption is established, according to the definition of instantaneous equivalent fuel consumption and the instantaneous optimization algorithm. On this basis, the SIMULINK model which can be integrated into the vehicle control model is established.

(2) Three actual driving conditions of the HEB can be obtained by the statistics, according to the operating data of hybrid electric buses. In the future, they can be used as vehicle driving cycles for the HEB simulation.

(3) The optimal engine torque and motor torque can be obtained by solving the objective function of instantaneous equivalent fuel consumption at the present moment. Based on the logic threshold torque distribution control strategy and the optimal torque of the engine and motor, the optimized torque distribution control strategy can be designed.

The remainder of this paper is structured as follows: Section II describes the design of the actual driving conditions. In Section III, based on instantaneous optimization algorithm, the torque distribution control strategy is presented and applied to the run of HEBs. Its comparisons with logic threshold torque distribution control strategy and simulation result analysis are conducted in Section IV. In Section V, conclusions and further research topics are presented.

II. DESIGN OF ACTUAL DRIVING CONDITIONS

According to the characteristics of bus driving conditions, it is necessary to develop a suitable road test, collect and analyze the data [23], [24]. The flow chart of the data collection, collation, and analysis is shown in Fig.1.

A. DATA COLLECTION OF THE ACTUAL DRIVING CONDITION

The paper selects a hybrid power bus which has the fixed route. Driving conditions of HEB have certain regularity [25]. The process of collecting data is as follows

Step 1: the experimental vehicle is selected with better condition.

Step 2: the real driving data is collected by CANOE data collector, which is the abbreviation of the CAN open environment. It is a bus development environment developed

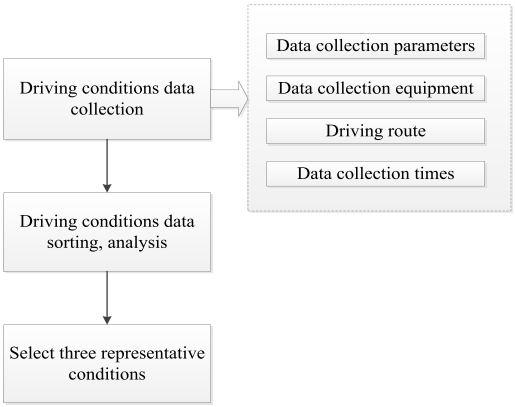

FIGURE 1. Flow chart of driving condition data collection, sorting, analysis.

by vector company of Germany, and is mainly designed for the development of automotive buses. The sampling time is set to 0.01s, and the main data acquisition includes: vehicle speed, time, acceleration, deceleration, SOC value, the engine operating point distribution in each stall and so on.

Step 3: the duration of the data collection is a month, the data collection starts at 6 a.m. and ends at 8 p.m., and the collected data has 400 hours of the accumulated time and 480 sets of data.

According to the changes of vehicle load, three kinds of actual driving conditions are analyzed from the collected data. They are divided into light load smooth (average 15 people), middle load slow heavy traffic (average 30 people) and heavy load congestion (average 60 people) [26]. The average values of the parameters are shown in Tab.1 under the three load conditions.

B. DATA ANALYSIS OF THE ACTUAL DRIVING CONDITION

According to analysis results of thirty groups, we can see that the average speed of light load is higher, which can reach 17km/h. In the case of heavy load condition, the average speed is only 10km/h. In the running data of a week, the proportion of light load condition is 39%, the proportion of the middle load condition is about 31%, and the proportion of the heavy load condition is 30%. And heavy load conditions are mainly in the morning and evening.

Actual operating characteristic parameters of three conditions of HEB are shown in Table 1. Statistical analysis can get curves that the actual operating speed of the vehicle can change with time under three conditions, including the light load, middle load and heavy load, see Fig. 2, 3 and 4.

The current driving state can be obtained by characteristic parameters of the Table 1 and speed curves under different conditions. Based on these typical conditions, the optimal energy control strategy is simulated.

III. TORQUE DISTRIBUTION CONTROL STRATEGY BASED ON INSTANTANEOUS OPTIMIZATION ALGORITHM

Among control strategies of hybrid electric vehicles, the adopted instantaneous optimization algorithm is used to optimize the output torque of the engine and the motor,

TABLE 1. Actual operating characteristic parameter of HEBs.

Condition	Max speed/ km	Average Speed/ (km/h)	Working time/s	Idle time/s	Average acceleration /(m.s^2)	Average deceleration /(m.s^2)	Max demand power/ kW
Light load	54.3	16.9	1897	97	0.362	-0.342	118
Middle load	50.9	12.4	2630	267	0.317	-0.257	101
Heavy load	48.3	9.57	3678	500	0.339	-0.223	144

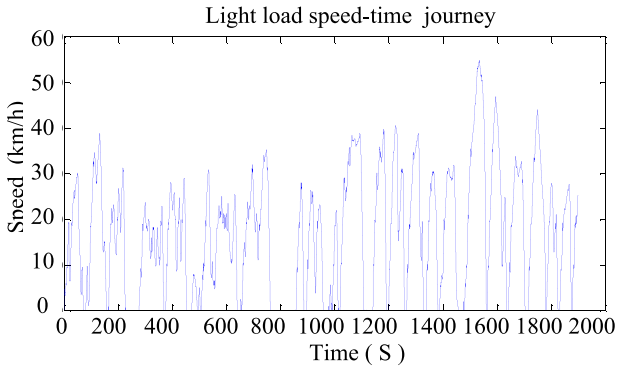

FIGURE 2. Speed change curve under the light load condition.

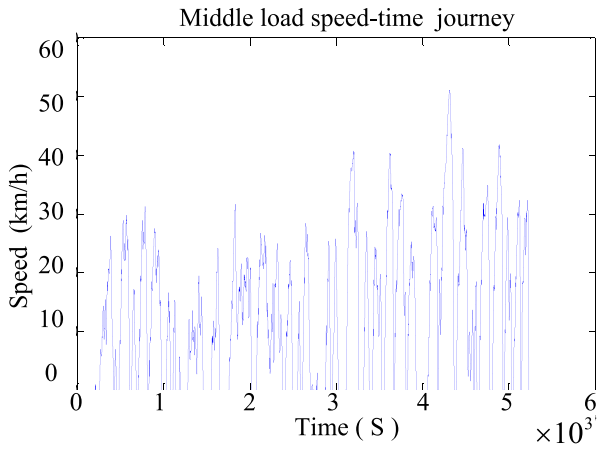

FIGURE 3. Speed change curve under the middle load.

so that fuel consumption of the power assembly is minimized at each moment [27]. Generally, the objective function of instantaneous equivalent fuel consumption is established. Then, the minimum value of the objective function is obtained. Finally, the output torque of engine and motor is obtained [28]. Based on the above concepts, the process of this study is shown in the Fig. 5.

A. OBJECTIVE FUNCTION OF THE INSTANTANEOUS EQUIVALENT FUEL CONSUMPTION

The instantaneous optimization algorithm is the instantaneous optimized output torque of the engine and motor so that each moment fuel consumption of vehicle power assembly can reach the minimum value[29], [30]. The instantaneous equivalent fuel consumption is described by the objective

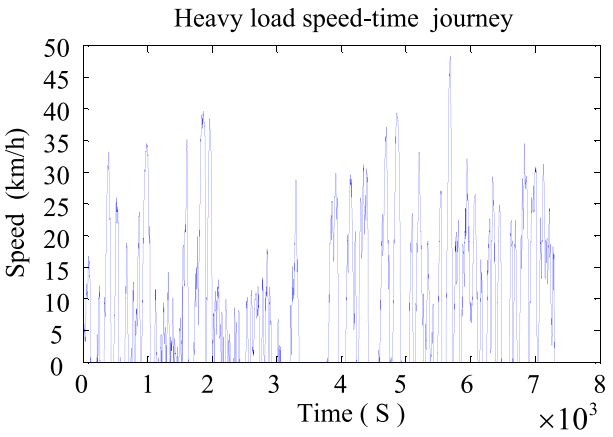

FIGURE 4. Speed change curve under the heavy load.

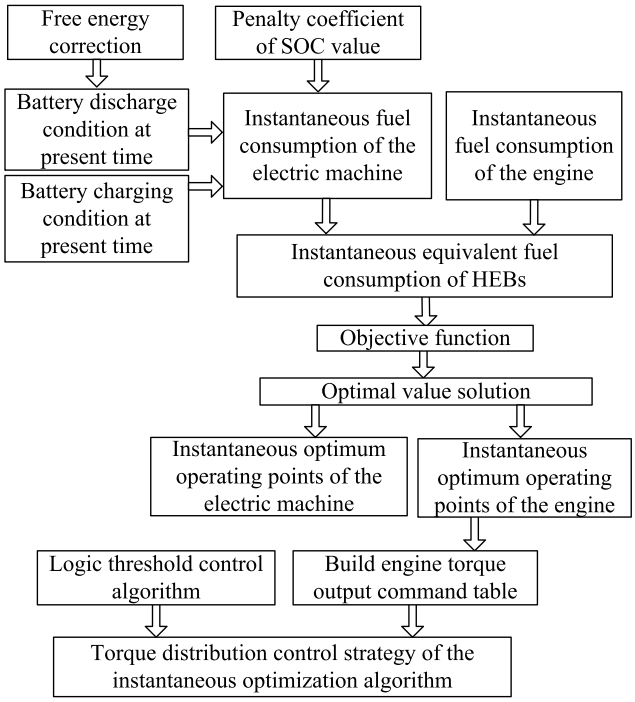

FIGURE 5. Flow process diagram of the torque distribution control strategy based on instantaneous optimization algorithm.

function [31]–[33].

$$J_{\min} = \sum_{t=0}^{N-1} Min\{\dot{m}_{fc}(T_{fc}(t), \omega_{fc}(t)) \cdot \Delta t + \dot{m}_{mc\_eq}(T_{mc}(t), \omega_{mc}(t)) \cdot \Delta t\} \quad (1)$$

TABLE 2. Basic parameters of HEBs.

Component	Descriptions
Engine	Product model: CA6SE1-21E3N Rated power / rated speed: 158kW/2300rpm Maximum torque: 700nm/1400rpm
Electric machine	Peak / rated power (kW): 90/30 Peak / rated speed (RPM): 6000/3600 Peak torque (nm): 220 Rated efficiency (%): 89
Battery	Lithium titanate, capacity: 40 [Ah], voltage:336 [V]
Vehicle	Length: 12 [m], empty mass: 18000 [kg]

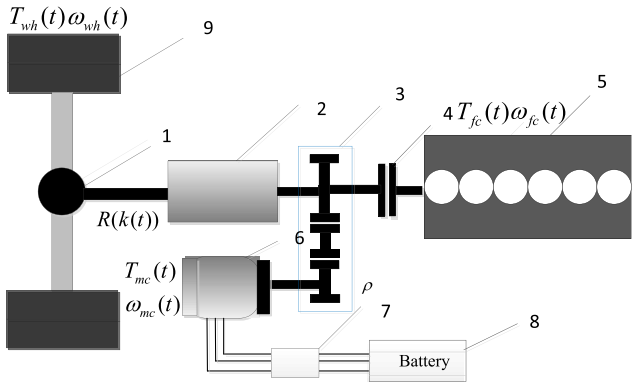

FIGURE 6. HEB structure diagram.

B. INSTANTANEOUS EQUIVALENT FUEL CONSUMPTION CALCULATION

According to the usage of battery, the equivalent fuel consumption can be divided into two kinds of operating conditions at the current time of the battery discharge and charge. Basic operating route parameters of HEB are shown in Table 2 [34], [35]. The formula of the instantaneous equivalent fuel consumption is separately calculated under the two kinds of conditions [36], [37]. The HEB structure diagram is shown in Fig.6.

where fc is the engine, mc is the motor, wh is the wheel, k is the number of shift, T is the torque; ω is the speed, gb is the gear-box, $R(k(t))$ is the transmission ratio of the main gear reducer and transmission gear box when the number of shift is k, ρ is the ratio of motor speed to transmission input shaft, η is the efficiency, and t is the runtime. The full name of AMT is automated mechanical transmission.

According to the mechanical connection among components, the rotational speed relationship is:

$$\omega_{wh}(t) = \omega_{fc}(t)/R(k(t)) = \omega_{mc}(t)/R(k(t)) = \omega_{mc}(t)/R(k(t)) \cdot \rho \quad (2)$$

The torque relationship is:

$$T_{wh}(t) = R(k(t)) \cdot (\rho \cdot T_{mc}(t) + T_{fc}(t)) \cdot \eta_{gb} \quad (3)$$

where the efficiency η_{gb} is determined by the torque of the positive and negative.

Due to the limitation of mechanical connection, torque conditions are as follows.

$$0 < T_{fc}(t) < T_{fc\_max} \quad (4)$$

$$T_{mc\_min} < T_{mc}(t) < T_{mc\_max} \quad (5)$$

Because the speed is also limited by the mechanical connection, the conditions are as follows.

$$\omega_{fc\_min} < \omega_{fc}(t) < \omega_{fc\_max} \quad (6)$$

$$0 < \omega_{mc}(t) < \omega_{mc\_max} \quad (7)$$

One of control strategy functions is to keep the balance of battery power as much as possible. Therefore, there is the following relationship.

$$SOC_{final} - SOC_{initial} \cong 0 \quad (8)$$

At every sampling time t, $\omega_{wh}(t)$ will be detected. $T_{wh}(t)$ is the demand torque signal of the wheel which is calculated through the given demand torque signal of the accelerator pedal [38].

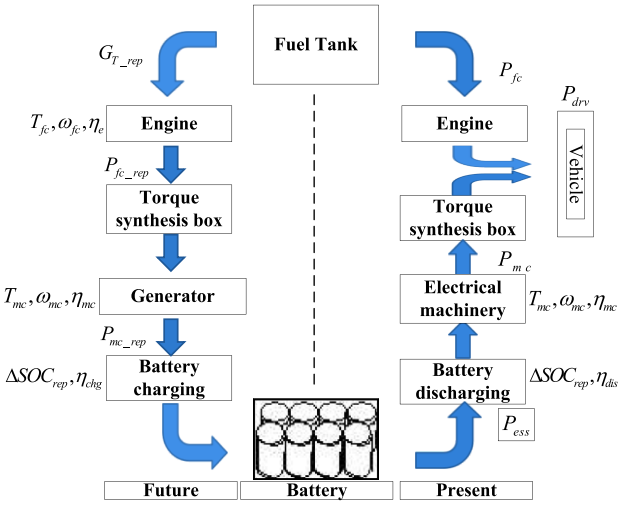

FIGURE 7. Energy flow Schematic diagram of battery power energy in the future.

1) BATTERY DISCHARGE CONDITION AT PRESENT TIME

The battery discharges at the current moment, and the battery charges for a period of time in the future. Fig.7 shows the battery energy flow. The present represents the current state of the battery work. The future is expressed to maintain the balance of the SOC value.

where T is torque, ω is speed, η_e is the work efficiency of the engine, η_{mc} is the working efficiency of the motor, η_{chg} is the battery charging efficiency, η_{dis} is the battery discharge efficiency, and P_{drv}, P_{fc}, P_{mc}, P_{mc_rep}, P_{ess} are respectively the demanded power, engine output power, power assisted motor power, the power of motor power generation, the battery output power.

The power battery provides some power to propel the vehicle forward at the sampling instant t. At the same time, the remaining power is provided by converting fuel into

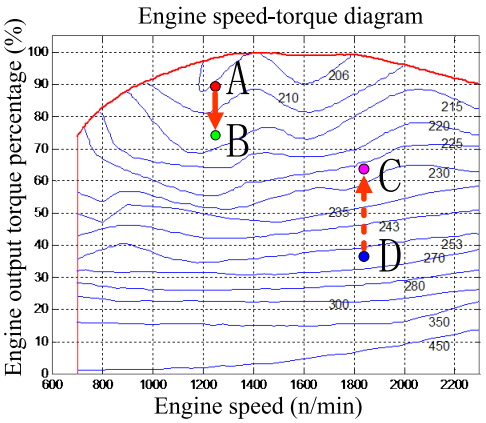

FIGURE 8. Schematic diagram of the engine working point in the current state of the battery.

heat energy from the main fuel tank of the engine. In the current state of the battery power generation, the schematic diagram of the engine operating point change is shown in Fig.8.

The required driver power is P_{drv}. When the battery is discharged, the motor is in the state of electric power, and the driver's demand power is shared by the engine and motor. Due to the motor involvement, the engine operating point decreases from A to B. According to characteristics of compressed natural gas (CNG) engine, the instantaneous fuel consumption rate is increased. But the motor energy conversion efficiency is higher, and the overall fuel consumption is reduced. In the future, when the battery is charged, the engine operating point increases from D to C. Thus, the fuel consumption rate is reduced. It is beneficial to make the engine work in the high efficiency area. There must be an intersection in the two contradictory states. Under the condition of keeping the balance of SOC value, the instantaneous equivalent fuel consumption is the lowest. This establishes a more explicit direction and target for establishing and solving the objective function of instantaneous equivalent fuel consumption [39], [40].

Under current discharge conditions, the instantaneous equivalent fuel consumption is calculated as follows. In the future of a control cycle, when the battery is charged, the engine output power is P_{fc0}, which expresses the engine power when the engine independently demands power. The instantaneous fuel consumption rate of the engine is b_{e0}. During the battery charging, engine operating points rise. At this time, the engine power is P_{fc1}, and instantaneous fuel consumption rate is b_{e1}. Then, the motor power P_{mc_rep} is negative for the generation state.

By the demand power of the vehicle, the relationship between the engine output power and motor output power is:

$$P_{fc0} = P_{fc1} + P_{mc\_req} = P_{drv} \tag{9}$$

According to the formula (9), b_{e0} and b_{e1}, the instantaneous fuel consumption rate of the motor can be derived from the motor (compensation) charging power P_{mc_rep}.

$$\begin{aligned} b_{e\_rep} &= \frac{(P_{fc1}b_{e1} - P_{fc0}b_{e0})\Delta t/3600}{P_{mc\_rep}\Delta t/3600} \\ &= \frac{P_{fc1}b_{e1} - P_{fc0}b_{e0}}{P_{mc\_rep}} \end{aligned} \tag{10}$$

The instantaneous fuel consumption of the motor can be obtained by the formula (10) and P_{mc_rep}.

$$\dot{m}_{rep} = \frac{b_{e\_rep}P_{mc\_rep}}{1000} = \frac{P_{fc1}b_{e1} - P_{fc0}b_{e0}}{1000} \tag{11}$$

$$P_{fc0} = P_{fc1} + P_{mc\_rep} \tag{12}$$

The formula (12) is brought into the formula (11), we can obtain the formula (13).

$$\dot{m}_{rep} = \frac{P_{fc1}(b_{e1} - b_{e0}) - P_{mc\_rep}b_{e0}}{1000} \tag{13}$$

Assuming that the battery discharge capacity is ΔC at the current control cycle, according to the relationship among the power, current, voltage, and the efficiency of the motor and battery discharge efficiency, the current circulation power of battery can be got by the formula (14).

$$\Delta C = \frac{I\Delta t}{3600} = \frac{P_{mc}\Delta t}{3.6 \cdot \eta_{mc}\eta_{dis}U_{oc}} \tag{14}$$

In the next period of time (charge), we assume that at the power of the N control cycle, the power relationship is the formula (15) in the i control cycle.

$$P_{fc0\_i} = P_{fc1\_i} + P_{mc\_i} \tag{15}$$

In order to maintain the balance of the battery, the battery compensation and the battery discharging quantity are equal at the current control cycle. For each control cycle, the sum of the charge quantity of the battery is calculated in the N control cycle. The future compensation power ΔC_{ess_rep} is:

$$\Delta C_{ess\_rep} = \sum_{i=1}^{N} \Delta C_{ess\_rep\_i} = \sum_{i=1}^{N} \frac{P_{mc\_i}\eta_{mc\_i}\eta_{chg\_i}\Delta t}{3.6U_{OC}} \tag{16}$$

The instantaneous fuel consumption of the motor is m_{rep_i} during the i control period.

$$m_{rep\_i} = \frac{(P_{fc1\_i}b_{e1\_i} - P_{fc0\_i}b_{e0\_i})\Delta t}{3600} \tag{17}$$

The instantaneous fuel consumption of the motor within the N control cycle is:

$$m_{rep} = \sum_{i=1}^{N} m_{rep\_i} \tag{18}$$

When the battery is compensated in the N control period, the equivalent fuel consumption rate of the motor is:

$$b_{mc\_eq} = \frac{m_{rep}}{P_{mc}\Delta t/3600} = \frac{\sum_{i=1}^{N}(P_{fc1\_i}b_{e1\_i} - P_{fc0\_i}b_{e0\_i})}{P_{mc}} \tag{19}$$

ΔC is obtained by the formula (14) and (16).

$$\Delta C = \frac{I \cdot \Delta t}{3600} = \frac{P_{mc}\Delta t}{3.6 \cdot \eta_{mc}\eta_{dis}U_{OC}} = \sum_{i=1}^{N} \frac{P_{mc\_i}\eta_{mc\_i}\eta_{chg\_i}\Delta t}{3.6U_{oc}} \quad (20)$$

The relationship between the discharge power P_{mc} at the current time and charge power of the next N control cycle is given by the formula (21).

$$\sum_{i=1}^{N} P_{mc\_i} = \frac{P_{mc}}{\eta_{mc}\eta_{dis}\bar{\eta}_{mc}\bar{\eta}_{chg}} \quad (21)$$

where η_{mc} and η_{dis} are respectively the motor efficiency and battery discharge efficiency at present time. $\bar{\eta}_{mc}$ and $\bar{\eta}_{chg}$ are respectively the average efficiency of the motor and the average charge efficiency of the battery in the N control period.

The formula (19) can be turned into the formula (22).

$$b_{mc\_eq} = \frac{\sum_{i=1}^{N}(P_{fc1\_i}b_{e1\_i} - P_{fc0\_i}b_{e0\_i})}{\eta_{mc}\eta_{dis}\bar{\eta}_{mc}\bar{\eta}_{chg}\sum_{i=1}^{N} P_{mc\_i}} \quad (22)$$

The formula (22) is simplified below.

$$b_{mc\_eq} = \frac{\bar{b}_{chg}}{\eta_{mc}\eta_{dis}\bar{\eta}_{mc}\bar{\eta}_{chg}} \quad (23)$$

where $\bar{b}_{chg} = \frac{\sum_{i=1}^{N}(P_{fc1\_i}b_{e1\_i} - P_{fc0\_i}b_{e0\_i})}{\sum_{i=1}^{N} P_{mc\_i}}$.

Finally, when the battery discharges at the current condition, the equivalent fuel consumption rate of the motor is:

$$\dot{m}_{mc\_eq} = \frac{\bar{b}_{chg}P_{mc}}{1000\eta_{mc}\eta_{dis}\bar{\eta}_{mc}\bar{\eta}_{chg}} \quad (24)$$

2) BATTERY CHARGING CONDITION AT PRESENT TIME

Fig.7 shows that the battery is charged at the current time, and discharged at a certain period of time in the future. Finally, it can balance the SOC value. Due to the participation of the motor, fuel consumption is reduced. In order to be consistent with the power symbol of the battery discharge, the equivalent fuel consumption is negative in the case of battery discharge [41], [42]. The energy flow diagram of battery power consumption conditions in the future and the diagram of the engine operating point changes at the current time of the battery charge are shown in Fig.7.

At the sampling time t, the battery provides partial power for propelling the vehicle forward, while the remaining power is supplied by the engine. The diagram of the engine operating point changes at the current time of the battery charge is shown in Fig.9. Under current charging conditions, the instantaneous equivalent fuel consumption is calculated as follows.

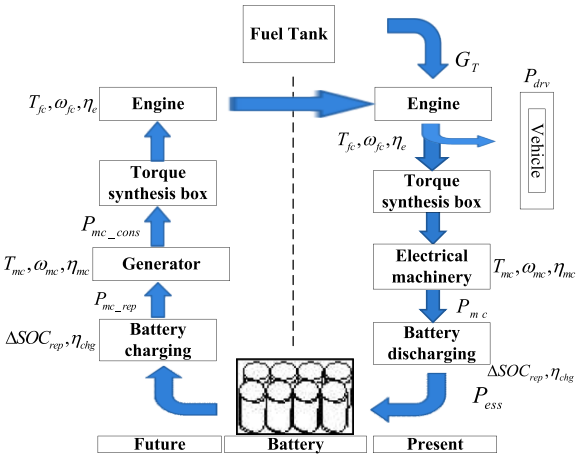

FIGURE 9. Energy flow diagram of battery power consumption conditions in the future.

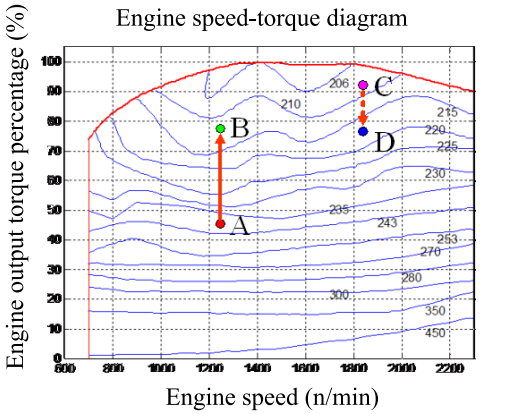

FIGURE 10. Diagram of the engine operating point changes at the current time of the battery charge.

Current driver's power demand for vehicles is P_{drv}. When the battery is charged at the present time, the motor is in the state of power generation. Because the driver's demand power and the power of the charge battery are supplied by the engine, the engine operating point increases from A to B. According to characteristics of CNG engine, the instantaneous fuel consumption is reduced, and the engine operating point moves toward the high efficiency zone.

In the future, the motor enters the joint drive mode, or the vehicle starts from the idle mode. Meanwhile, the battery is discharged. The engine operating point decreases from D to C, and fuel consumption is increased, as shown in Fig.10. But the consumption of electric energy can be compensated by the high conversion rate of electric energy when the motor is driven. There is a certain intersection point between the two kinds of battery. Under the condition of keeping the balance of SOC value, the instantaneous equivalent fuel consumption is the lowest [43].

At the present time, the engine output power is $P_{fc2}(T_2, \omega_2)(P_{fc2} = P_{drv})$, and the instantaneous fuel consumption rate of the engine is b_{e2}. Due to the battery charging, engine operating points rise. At this time, the engine power

is $P_{fc3}(T_3, \omega_2)(P_{fc3} > P_{drv})$, and the instantaneous fuel consumption rate is b_{e3}. Because the motor is under the state of power generation, the motor torque $P_{mc\_chg}(P_{mc\_chg} < 0)$ is negative at this time.

Due to the fact that vehicle demands power, the relationship between the engine output power and motor output power is:

$$P_{fc2} = P_{fc3} + P_{mc\_chg} = P_{drv} \tag{25}$$

According to the formula (25), b_{e2}, and b_{e3}, the instantaneous fuel consumption rate of the motor is derived when the motor charging power is P_{mc_chg}.

$$\begin{aligned} b_{e\_chg} &= \frac{(P_{fc3}b_{e3} - P_{fc2}b_{e2})\Delta t/3600}{P_{mc\_chg}\Delta t/3600} \\ &= \frac{P_{fc3}b_{e3} - P_{fc2}b_{e2}}{P_{mc\_chg}} \end{aligned} \tag{26}$$

The instantaneous fuel consumption of the motor can be obtained by the formula (26) and P_{mc_chg}.

$$m_{chg} = \frac{(P_{fc3}b_{e3} - P_{fc2}b_{e2})\Delta t}{3600} \tag{27}$$

The battery charging capacity is ΔC at the current control cycle. According to the relationship among the power, current and power, and voltage, considering the efficiency of the motor and the battery charge efficiency, the current control cycle battery charge ΔC can be attained.

$$\Delta C_{ess\_chg} = \frac{I \cdot \Delta t}{3600} = \frac{P_{mc\_chg}\eta_{mc}\eta_{chg}\Delta t}{3.6U_{OC}} \tag{28}$$

In order to maintain the balance of battery power, the battery consumption is equal to the battery charge at the current control cycle in the future. For each control cycle, the sum of the discharge quantity of the battery is calculated in the N control cycle. It can get the future compensation power ΔC_{ess_consum}.

$$\Delta C_{ess\_consum} = \sum_{i=1}^{N} \frac{P_{mc\_i}\Delta t}{3.6\eta_{mc\_i}\eta_{dis}U_{OC}} \tag{29}$$

Assuming that the formula (28) and formula (29) are equal, we can get the motor power.

$$\sum_{i=1}^{N} P_{mc\_i} = P_{mc\_chg}\eta_{mc}\eta_{chg}\bar{\eta}_{mc}\bar{\eta}_{dis} \tag{30}$$

where η_{mc} and η_{chg} are respectively the motor efficiency and battery charging efficiency at the current time; $\overline{\eta}_{mc}$ and $\overline{\eta}_{dis}$ are respectively the average efficiency of the motor and the average discharge efficiency of the battery at the N control cycle.

By formula (27) and formula (30), we can get the equivalent fuel consumption rate of battery power consumption can be got in the future.

$$b_{mc\_eq} = \frac{(P_{fc3}b_{e3} - P_{fc2}b_{e2})\Delta t/3600}{\sum_{i=1}^{N} P_{mc\_i}\Delta t/3600} \tag{31}$$

The above type can be decomposed as the next type.

$$b_{mc\_eq} = \frac{(P_{fc3}b_{e3} - P_{fc2}b_{e2})}{P_{mc\_chg}\eta_{mc}\eta_{chg}\bar{\eta}_{mc}\bar{\eta}_{dis}} \tag{32}$$

$$b_{mc\_eq} = \frac{b_{mc\_chg}}{\eta_{mc}\eta_{chg}\bar{\eta}_{mc}\bar{\eta}_{dis}} \tag{33}$$

where $b_{mc\_chg} = \frac{P_{fc3}b_{e3} - P_{fc2}b_{e2}}{P_{mc\_chg}}$.

When the battery is charged at the present time, the instantaneous equivalent fuel consumption calculation formula of the motor is:

$$\dot{m}_{mc\_eq} = \frac{b_{mc\_chg}P_{mc\_chg}}{1000\eta_{mc}\eta_{chg}\bar{\eta}_{mc}\bar{\eta}_{dis}} \tag{34}$$

C. RECOVERY OF REGENERATIVE BRAKING ENERGY AND SLIDING ENERGY

In the power generation mode, the engine is provided the demand power of the vehicle, while the battery is charged at the same time. The battery can also be recovered by the recovering of sliding and braking energy [44]. In order to maintain the battery power balance, the energy consumption of the battery needs to be modified in the process which establishes the objective function.

$$\bar{P}_{motorbrake}(t) = \frac{\sum_{j=1}^{M_{\text{mod }e\_7}} P_{motorbrake}\Delta t}{M_{\text{mod }e\_1}\Delta t} \tag{35}$$

$$\bar{P}_{coastchage}(t) = \frac{\sum_{j=1}^{M_{\text{mod }e\_6}} P_{coastch\,arg\,e}\Delta t}{M_{\text{mod }e\_1}\Delta t} \tag{36}$$

where $M_{\text{mode\_1}}$, $M_{\text{mode\_6}}$ and $M_{\text{mode\_7}}$ are respectively the action time segments in the joint drive, sliding charge and brake energy operation mode.

The braking and sliding segments of the vehicle are not predictable in the driving process. To calculate the motor power, the compensation energy of the battery should be considered at the braking and coasting fragment when the vehicle is in the joint drive model. Thus, the correction of energy consumption of the battery can be completed. Under the modified current discharge condition, the instantaneous equivalent fuel consumption functions of the motor are the formula (41) and (42).

$$\dot{m}_{mc\_eq}(P_{mc}(t)) = \frac{\bar{b}_{chg}(P_{mc}(t) + \bar{P}_{motorbrake} + \bar{P}_{motorcoast})}{1000\eta_{mc}(t)\eta_{dis}(t)\bar{\eta}_{mc}\bar{\eta}_{chg}} \tag{37}$$

$$\dot{m}_{mc\_eq}(P_{mc\_chg}) = \frac{b_{mc\_chg}P_{mc\_chg}}{1000\eta_{mc}(t)\eta_{chg}(t)\bar{\eta}_{mc}\bar{\eta}_{chg}} \tag{38}$$

where $\bar{b}_{chg}$ and b_{mc_chg} are respectively the average fuel consumption rate of the battery charge in the n control period of the future under the current discharge condition and the fuel consumption rate of battery charging at current time of battery charging condition. $\bar{b}_{chg}$ and b_{mc_chg}

TABLE 3. Average fuel consumption rate under three typical operating conditions of energy correction.

Power / Condition	$\overline{P}_{motorbrake}$ (w)	$\overline{P}_{motorcoast}$ (w)	$\overline{b}_{cyc\_chg}$ (g/(kW.h))
Light load	-87.9056	-35.6391	39.123
Middle load	-54.9115	-35.2442	46.8
Heavy load	-39.1554	-20.2857	46.97

are approximately replaced by the average fuel consumption rate $\overline{b}_{cyc\_chg}$. Table 3 lists results of the simulation of the original car under three typical operating conditions, which includes the regeneration power of the braking energy, the energy of the sliding charge, and the average fuel consumption rate of the battery compensation conditions.

D. OBJECTIVE FUNCTIONS OF THE INSTANTANEOUS EQUIVALENT FUEL CONSUMPTION

1) ESTABLISHMENT OF THE OBJECTIVE FUNCTION

The formula (37) and (38) can be changed into the following forms.

$$\dot{m}_{mc\_eq}(P_{mc}(t)) = \frac{\bar{b}_{cyc_chg}(P_{mc}(t)+\bar{P}_{motorbrake}+\bar{P}_{motorcoast})}{1000\eta_{mc}(t)\eta_{dis}(t)\bar{\eta}_{mc}\bar{\eta}_{chg}} \tag{39}$$

$$\dot{m}_{mc\_eq}(P_{mc\_chg}) = \frac{b_{cyc_chg}P_{mc\_chg}}{1000\eta_{mc}(t)\eta_{chg}(t)\bar{\eta}_{mc}\bar{\eta}_{chg}} \tag{40}$$

where $\overline{P}_{motorbrake}$ is the amendment power of the battery energy consumption under the regenerative braking mode. $\overline{P}_{motorcoast}$ is the amendment power of the battery energy consumption in the sliding mode.

Simultaneous hypothesis,

$$f_{eq\_dis} = \frac{\bar{b}_{cyc_chg}}{\bar{\eta}_{mc}\bar{\eta}_{chg}} \tag{41}$$

$$f_{eq\_dis} = \frac{\bar{b}_{cyc_chg}}{\bar{\eta}_{mc}\bar{\eta}_{dis}} \tag{42}$$

The general expression of the instantaneous equivalent fuel consumption control algorithm is:

$$J_{\min} = \sum_{t=0}^{N-1} Min\{\dot{m}_{fc}(T_{fc}(t), \omega_{fc}(t))\Delta t + \dot{m}_{mc}(T_{mc}(t), \omega_{mc}(t))\Delta t\} \tag{43}$$

The expression form of the torque speed becomes the power, and the deformation is the formula (44).

$$J_{\min} = \sum_{t=0}^{N-1} Min\{\dot{m}_{fc}(T_{fc}(t) + \dot{m}_{mc\_eq}(P_{mc}(t)))\Delta t/3600\} \tag{44}$$

where $\lambda = \frac{1+sign(P_{mc}(t))}{2}$.

$$f_{eq\_dis} = \frac{\bar{b}_{cyc_chg}}{\bar{\eta}_{mc}\bar{\eta}_{chg}}$$

$$f_{eq\_dis} = \frac{\bar{b}_{cyc_chg}}{\bar{\eta}_{mc}\bar{\eta}_{dis}}$$

$$\dot{m}_{mc\_eq}(P_{mc}(t)) = \lambda f_{eq\_dis}\frac{P_{mc}(t)+\bar{P}_{motorbrake}+\bar{P}_{motorcoast}}{1000\eta_{mc}(t)\eta_{dis}(t)} + (1-\lambda)f_{eq\_chg}\frac{P_{mc}(t)}{1000\eta_{mc}(t)\eta_{chg}(t)} \tag{45}$$

The final expression of the instantaneous equivalent fuel consumption control algorithm is as follows in this paper.

$$J_{\min} = \sum_{t=0}^{N-1} Min\{(\dot{m}_{fc}(P_{fc}(t)))K_{soc}(\lambda f_{eq\_dis} \times \frac{P_{mc}(t)+\bar{P}_{motorbrake}+\bar{P}_{motorcoast}}{1000\eta_{mc}(t)\eta_{dis}(t)} + (1-\lambda)f_{eq\_chg} \times \frac{P_{mc}(t)}{1000\eta_{mc}(t)\eta_{chg}(t)}) + \Delta t/3600\} \tag{46}$$

2) OBJECTIVE FUNCTION SOLUTION OF THE OPTIMAL VALUE

The optimal solution of the objective function is obtained by the method of nonlinear programming, and the power allocation ratio is determined. General constrained nonlinear programming problems are described the formula (47).

$$\min_{x.s.t.G(x)\le 0} F(x) \tag{47}$$

where $x = [x_1, x_2, \cdots, x_n]^T$ is a set of vectors. Under the condition of satisfying the constraint condition $G(x) \le 0$, the objective function $F(x)$ is minimized. At this time, the X is the optimal solution.

In the MATLAB optimization toolbox, fmincon( ) is devoted to solving optimization problems of the constrained nonlinear function. The specific call format of the function is:

$$[x, fval, ecitflag, output] = f\min con(fun, x0, A, b, Aeq, beq, lb, ub, nonlc, options) \tag{48}$$

where fun is the object function, x0 is the initial value, nonlc is nonlinear constraint conditions, options is optimization options (generally default), x is the value which is obtained by the optimization function. If exitflag > 0, x is the solver, or x is not the final solver which is only the value of the optimization process when the iteration is stopped. The fval is the value of the objective function for solving x, exitflag is the description launch condition, exitflag > 0 expresses the objective function that converges to the solution x, exitflag $= 0$ expresses the maximum number of function evaluation or iteration, exitflag < 0 expresses the objective function which does not converge. The output contains the optimization result information: Iteration is iterations, Algorithm is the adopted algorithm, and FuncCount is the number of evaluation times.

E. CORRECTION METHOD OF THE SOC VALUE

K_{soc} is the penalty coefficient of SOC value. The SOC value of the battery is divided into the lower limit value, best value and upper limit value. When the SOC value of the battery is near the optimum value, K_{soc} is near 1, or K_{soc} is gradually increasing. At present, there are two kinds of mathematical expressions for the SOC value penalty coefficient of the battery. One is the tangent function [45], the other is a piecewise function of the coupling between the cubic curve and quartic curve [46]. According to the change trend of the SOC value in the actual operation process, the piecewise function, which is the coupling of the three curve and the four curve, is more suitable. Because the driving operating conditions of the hybrid bus change more often in the driving process, starting and stopping frequently, the chance of the vehicle entering the charge mode is rare. By adjusting the parameters of the penalty coefficient curve during the SOC value of the second kinds of batteries, the optimal value and the upper limit value of the battery SOC value change relatively more smooth. However, SOC value change changes dramatically at the near lower limit value. Thus, the SOC value can be maintained better in the range of high efficiency at the charge and discharge status, and avoid the situation of the low battery power [47].

The expression form of the piecewise function, which is formed by the coupling of the cubic curve and quartic curve, is the formula (35).

$$DEV_{soc} = SOC - \frac{SOC_{lo} + SOC_{hi}}{2} \tag{49}$$

$$K_{soc} = f(DEV_{soc}) = a + bDEV_{soc}^3 + cDEV_{soc}^4 \tag{50}$$

where DEV_{soc} is the size of the SOC value which deviates from the optimum value. SOC_{lo}, SOC_0 and SOC_{hi} are respectively the lower limit value, the best value and the upper limit value of the SOC value. According to the need, a, b, and c can select the appropriate coefficient.

When $DEV_{soc} \geq 0$

$$K_{soc} = 1 - 900DEV_{soc}^3 \tag{51}$$

When $DEV_{soc} < 0$,

$$K_{soc} = -900 - 100DEV_{soc}^3 + 8000DEV_{soc}^4 \tag{52}$$

IV. MODELING AND SIMULATION

According to the HEB structure, the vehicle model is built in the Cruise software and shown in Fig.11 [48]. Based on torque distribution control strategy, the Simulink model of the instantaneous optimization algorithm is integrated into the whole vehicle controller by the Interface and Cruise software. Through the joint simulation, the simulation is carried out on three typical cases of light load, middle load and heavy load, as shown in Fig.12 to Fig.14. Gas consumption results are shown in Table 4.

Simulation results demonstrate the torque distribution control strategy of the instantaneous optimization algorithm can

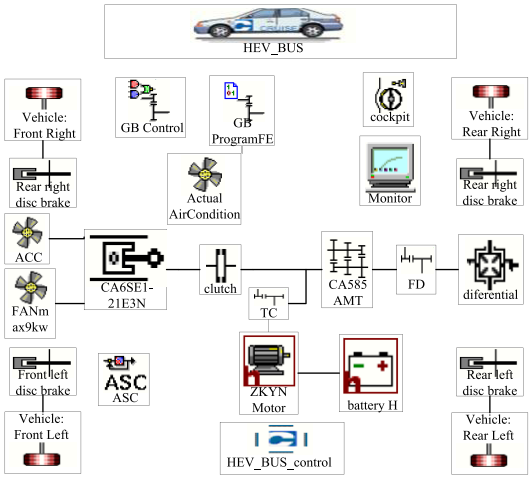

FIGURE 11. Structure diagram of HEB control model.

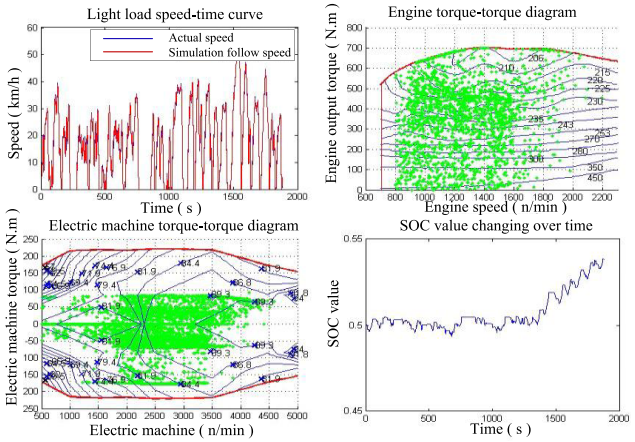

FIGURE 12. Simulation results of the instantaneous optimization algorithm-light load condition.

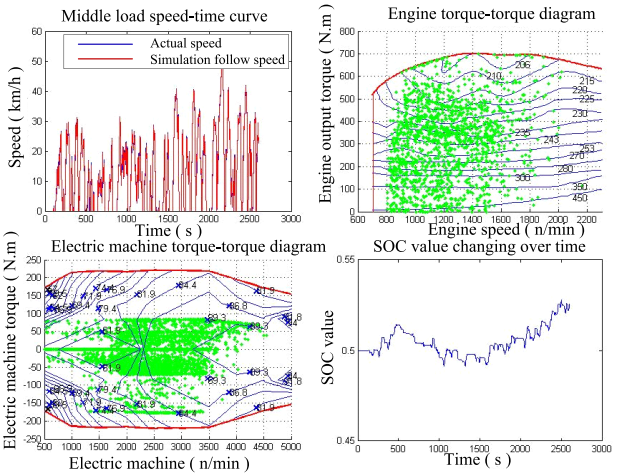

FIGURE 13. Simulation results of the instantaneous optimization algorithm-middle load condition.

effectively limit the engine and motor operating points in the high efficiency area. Combining the simulation speed with the actual speed of the vehicle, the vehicle dynamic performance

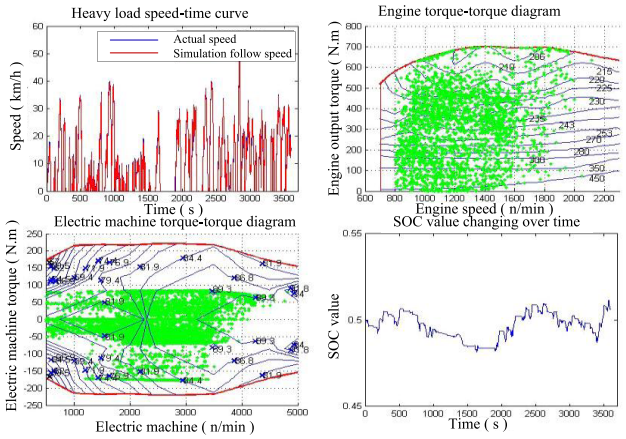

FIGURE 14. Simulation results of the instantaneous optimization algorithm-heavy load condition.

TABLE 4. Economic simulation results of the instantaneous optimization algorithm based on the torque distribution control strategy for different conditions.

Gas loss (m^3/100km) / Type	Light load	Middle load	Heavy load
Instantaneous optimization algorithm	36.84	42.84	50.55
Original torque distribution control	39.73	46.11	54.25
Reduce gas consumption rate (%)	7.27%	7.09%	6.82%

can be better guaranteed. Besides, the battery power can be well balanced. The HEB gas consumption is low, as shown in Table 4.

V. CONCLUSION

In order to reduce the gas consumption and maintain a good battery power balance, this paper adopts the instantaneous optimization algorithm to optimize the energy control strategy of HEB. Firstly, driving condition data of parallel HEB is collected and analyzed, and three kinds of representative driving conditions are obtained, which are respectively light load, middle load and heavy load. Secondly, objective functions of instantaneous equivalent fuel consumption are set up by the instantaneous optimal control algorithm. The objective function includes the current instantaneous oil consumption of engine and motor instantaneous fuel consumption. When instantaneous fuel consumption of the electric machine is analyzed, the condition of the present moment is divided into the current condition of battery power compensation and the current battery power consumption condition. The instantaneous fuel consumption equation of the electric machine is established on two kinds of working conditions. Meanwhile, in order to maintain the balance of the battery, fuel consumption items of the electric machine introduce "battery SOC value of penalty coefficient". The process of solving the objective function is attributed to the nonlinear objective function of linear programming problem. Then, considering actual driving conditions, and based on the objective function, the model of the instantaneous optimal control algorithm is established which is integrated into the vehicle model. Finally, the HEB instantaneous optimal control model is simulated under three representative driving conditions. Its application for the designed control model of HEBs is shown to demonstrate the proposed instantaneous optimal approach. Simulation result analysis and comparison of the fuel economy with the existing methods are performed. The results show that:

(i) Under three kinds of representative driving conditions, the simulation speed is close to the actual speed. It shows that the cycle conditions used in the simulation can be close to the actual driving state. It provides a real vehicle driving condition to verify the effectiveness of the vehicle energy control strategy.

(ii) As can be seen from the Fig.11, Fig.12, and Fig.13, the torque distribution control strategy, which is based on the instantaneous optimization algorithm, can effectively control operating points of the engine and electric machine in the high efficiency area. Work efficiency of the engine and electric machine are improved.

(iii) As can be seen from the Fig.11, Fig.12, and Fig.13, SOC value of the battery power can be well maintained in a certain range. The service life of the battery and the utilization ratio of the electric energy are improved by the instantaneous optimal control strategy.

(iv) Compared with the logic threshold value torque distribution control strategy, the torque distribution control strategy of the instantaneous optimization algorithm can effectively reduce gas consumption under the premise of ensuring the power of HEBs.

Future studies should focus on integrating the developed procedure of the HEB control model into a computer design support system for verifying the effectiveness of the designed control strategy by real vehicle tests [49]–[52]. Moreover, more advanced optimization algorithms need more in-depth theoretical research in the future [53], [34].

COMPETING INTERESTS

The authors declare that they have no competing interests.

REFERENCES

[1] H. Banvait, S. Anwar, and Y. Chen, "A rule-based energy management strategy for plug-in hybrid electric vehicle (PHEV)," in *Proc. Amer. Control Conf.*, Jun. 2009, pp. 3938–3943.

[2] Q. Tu, X. Zhang, M. Pan, C. Jiang, and J. Xue, "Design and optimization of the power management strategy of an electric drive tracked vehicle," *Math. Problems Eng.*, vol. 2016, Aug. 2016, Art. no. 6185743.

[3] A. Sciarretta and L. Guzzella, "Control of hybrid electric vehicles," *IEEE Control Syst.*, vol. 27, no. 7, pp. 60–70, Apr. 2007.
[4] Y. Liu *et al.*, "The road of new energy bus (part two)," *World Driver*, vol. 9, pp. 60–67, Dec. 2012.
[5] F. R. Salmasi, "Control strategies for hybrid electric vehicles: Evolution, classification, comparison, and future trends," *IEEE Trans. Veh. Technol.*, vol. 56, no. 5, pp. 2393–2404, Sep. 2007.
[6] V. Sezer, M. Gokasan, and S. Bogosyan, "A novel ECMS and combined cost map approach for high-efficiency series hybrid electric vehicles," *IEEE Trans. Veh. Technol.*, vol. 60, no. 8, pp. 3557–3570, Oct. 2011.
[7] J.-S. Won, R. Langari, and M. Ehsani, "An energy management and charge sustaining strategy for a parallel hybrid vehicle with CVT," *IEEE Trans. Control Syst. Technol.*, vol. 13, no. 2, pp. 313–320, Mar. 2005.
[8] J. Wu, C.-H. Zhang, and N.-X. Cui, "Fuzzy energy management strategy for a hybrid electric vehicle based on driving cycle recognition," *Int. J. Automotive Technol.*, vol. 13, pp. 1159–1167, Dec. 2012.
[9] Y. Zhou, S. Ou, J. Lian, and L. Li, "Optimization of hybrid electric bus driving system's control strategy," *Procedia Eng.*, vol. 15, pp. 240–245, Dec. 2011.
[10] X. Zeng *et al.*, "Multi-factor integrated parametric design of power-split hybrid electric bus," *J. Cleaner Prod.*, vol. 115, pp. 88–100, Mar. 2016.
[11] J. Kim, J. Shin, C. Chun, and B. H. Cho, "Stable configuration of a Li-Ion series battery pack based on a screening process for improved voltage/SoC balancing," *IEEE Trans. Power Electron.*, vol. 27, no. 1, pp. 411–424, Jan. 2012.
[12] L. Tribioli, R. Cozzolino, D. Chiappini, and P. Iora, "Energy management of a plug-in fuel cell/battery hybrid vehicle with on-board fuel processing," *Appl. Energy*, vol. 184, pp. 140–154, Dec. 2016.
[13] K. Ç. Bayindir, M. A. Gözüküçük, and A. Teke, "A comprehensive overview of hybrid electric vehicle: Powertrain configurations, powertrain control techniques and electronic control units," *Energy Convers. Manage.*, vol. 52, no. 2, pp. 1305–1313, 2011.
[14] Y. Haitao, Z. Yulan, L. Zunnian, and H. Kui, "LQR-based power train control method design for fuel cell hybrid vehicle," *Math. Problems Eng.*, vol. 2013, Oct. 2013, Art. no. 968203.
[15] H.-C. Liu, J.-X. You, Z. Li, and G. Tian, "Fuzzy petri nets for knowledge representation and reasoning: A literature review," *Eng. Appl. Artif. Intell.*, vol. 60, pp. 45–56, Jan. 2017.
[16] Z. Amjadi and S. S. Williamson, "Power-electronics-based solutions for plug-in hybrid electric vehicle energy storage and management systems," *IEEE Trans. Ind. Electron.*, vol. 57, no. 2, pp. 608–616, Feb. 2010.
[17] Q. Li, W. Chen, Y. Li, S. Liu, and J. Huang, "Energy management strategy for fuel cell/battery/ultracapacitor hybrid vehicle based on fuzzy logic," *Int. J. Elect. Power Energy Syst.*, vol. 43, no. 1, pp. 514–525, 2012.
[18] N. Kim, S. W. Cha, and H. Peng, "Optimal equivalent fuel consumption for hybrid electric vehicles," *IEEE Trans. Control Syst. Technol.*, vol. 20, no. 3, pp. 817–825, May 2012.
[19] A. Panday and H. Bansal, "Energy management strategy for hybrid electric vehicles using genetic algorithm," *J. Renew. Sustain. Energy*, vol. 8, no. 1, p. 015701, Jan. 2016.
[20] G. Becerra, L. Alvarez-Icaza, and A. Pantoja-Vázquez, "Power flow control strategies in parallel hybrid electric vehicles," *Proc. Inst. Mech. Eng. D, J. Automobile Eng.*, vol. 230, no. 14, pp. 1925–1941, 2016.
[21] K. Yi, J. Kim, K. Hwang, M. Lee, H. Kim, and I. S. Suh, "Operational efficiency comparison on Eco-friendly vehicles including dynamic wireless charging," *Int. J. Automotive Technol.*, vol. 16, pp. 1017–1030, Dec. 2015.
[22] X. Zhang and C. Mi, *Vehicle Power Management: Modeling, Control and Optimization*. London, U.K.: Springer, 2011.
[23] L. Li, S. You, C. Yang, B. Yan, J. Song, and Z. Chen, "Driving-behavior-aware stochastic model predictive control for plug-in hybrid electric buses," *Appl. Energy*, vol. 162, pp. 868–879, Jan. 2016.
[24] G. Tian, H. Zhang, M. Zhou, and Z. Li, "AHP, gray correlation, and TOPSIS combined approach to green performance evaluation of design alternatives," *IEEE Trans. Syst., Man, Cybern., Syst.*, to be published, doi: 10.1109/TSMC.2016.2640179.
[25] J. Lian, H. Han, L. Li, Y. Zhou, and J. Feng, "Research on optimal control method of hybrid electric vehicles," *Simul. Trans. Soc. Model. Simul. Int.*, vol. 89, no. 9, pp. 1137–1146, Sep. 2013.
[26] B. Yao, P. Hu, X. Lu, J. Gao, and M. Zhang, "Transit network design based on travel time reliability," *Transp. Res. C, Emerg. Technol.*, vol. 43, pp. 233–248, Jun. 2014.
[27] S. Delprat, T. M. Guerra, and J. Rimaux, "Control strategies for hybrid vehicles: Optimal control," in *Proc. 56th IEEE Veh. Technol. Conf.*, Sep. 2002, pp. 1681–1685.
[28] C.-C. Lin, H. Peng, J. W. Grizzle, and J.-M. Kang, "Power management strategy for a parallel hybrid electric truck," *IEEE Trans. Control Syst. Technol.*, vol. 11, no. 6, pp. 839–849, Nov. 2003.
[29] C. Yang, J. Song, L. Li, S. Li, and D. Cao, "Economical launching and accelerating control strategy for a single-shaft parallel hybrid electric bus," *Mech. Syst. Signal Process.*, vols. 66–77, pp. 649–664, Aug. 2016.
[30] G. Tian, J. Chu, H. Hu, and H. Li, "Technology innovation system and its integrated structure for automotive components remanufacturing industry development in China," *J. Cleaner Prod.*, vol. 85, pp. 419–432, Dec. 2014.
[31] D. J. Xuan, J. W. Kim, and Y. B. Kim, "Optimal operation strategy development for fuel cell hybrid vehicle," *J. Mech. Sci. Technol.*, vol. 25, pp. 183–192, Jan. 2011.
[32] Z. Lei and H. Xie, "Active regulation of battery charge-sustaining in ECMS: Application in energy management for engine waste heat recovery system," *Int. J. Automotive Technol.*, vol. 17, no. 6, pp. 1055–1065, 2016.
[33] J. P. Gao, G.-M. G. Zhu, E. G. Strangas, and F. C. Sun, "Equivalent fuel consumption optimal control of a series hybrid electric vehicle," *Proc. Inst. Mech. Eng. D, J. Automobile Eng.*, vol. 223, no. 8, pp. 1003–1018, 2009.
[34] C. Yang, L. Li, S. You, B. Yan, and X. Du, "Cloud computing-based energy optimization control framework for plug-in hybrid electric bus," *Energy*, vol. 125, pp. 11–26, Apr. 2017.
[35] L. Li, C. Yang, Y. Zhang, L. Zhang, and J. Song, "Correctional DP-based energy management strategy of plug-in hybrid electric bus for city-bus route," *IEEE Trans. Veh. Technol.*, vol. 64, no. 7, pp. 2792–2803, Jul. 2015.
[36] Q. L. Zhu, "Study on the control strategy of hybrid electric vehicle based on instantaneous optimization," M.S. thesis, Jilin Univ., Changchun, China, 2009.
[37] L. Serrao, S. Onori, and G. Rizzoni, "A comparative analysis of energy management strategies for hybrid electric vehicles," *J. Dyn. Syst., Meas., Control Trans.*, vol. 133, no. 3, p. 031012, 2011.
[38] B. Hannon, P. Sergeant, and L. Dupré, "Torque and torque components in high-speed permanent-magnet synchronous machines with a shielding cylinder," *Math. Comput. Simul.*, vol. 130, pp. 70–80, Dec. 2016.
[39] S. Delprat, J. Lauber, T. M. Guerra, and J. Rimaux, "Control of a parallel hybrid powertrain: Optimal control," *IEEE Trans. Veh. Technol.*, vol. 53, no. 3, pp. 872–881, May 2004.
[40] S. Delprat, T. M. Guerra, G. Paganelli, J. Lauber, and M. Delhom, "Control strategy optimization for an hybrid parallel powertrain," in *Proc. ACC*, Arlington, VA, USA, Jun. 2001, pp. 1315–1320.
[41] Z. Chen, W. Liu, W. Chen, and Y. Yang, "Online energy management of plug-in hybrid electric vehicles for prolongation of all-electric range based on dynamic programming," *Math. Problems Eng.*, vol. 2015, Nov. 2015, Art. no. 368769.
[42] Z. Chen, R. Xiong, K. Wang, and B. Jiao, "Optimal energy management strategy of a plug-in hybrid electric vehicle based on a particle swarm optimization algorithm," *Energies*, vol. 8, no. 5, pp. 3661–3678, 2015.
[43] A. Sciarretta, M. Back, and L. Guzzella, "Optimal control of parallel hybrid electric vehicles," *IEEE Trans. Control Syst. Technol.*, vol. 12, no. 3, pp. 352–363, May 2004.
[44] X. Cao and T. Ishikawa, "Optimum design of a regenerative braking system for electric vehicles based on fuzzy control strategy," *IEEJ Trans. Elect. Electron. Eng.*, vol. 11, no. S1, pp. S186–S187, 2016.
[45] G. Tian, M. Zhou, and J. Chu, "A chance constrained programming approach to determine the optimal disassembly sequence," *IEEE Trans. Autom. Sci. Eng.*, vol. 10, no. 4, pp. 1004–1013, Oct. 2013.
[46] W. Jiang and B. Fahimi, "Active current sharing and source management in fuel cell-battery hybrid power system," *IEEE Trans. Ind. Electron.*, vol. 57, no. 2, pp. 752–761, Feb. 2010.
[47] A. Soebandrio, R. T. Bambang, A. S. Rohman, C. J. Dronkers, R. Ortega, and A. Sasongko, "Energy management of fuel cell/battery/supercapacitor hybrid power sources using model predictive control," *IEEE Trans. Ind. Informat.*, vol. 10, no. 4, pp. 1992–2002, Nov. 2014.
[48] X. Zeng, Y. Yu, J. Wang, Q. Wang, and P. Y. Wang, "Modelling and simulation of active and synchronized gear-shift of hybrid electric bus based on CRUISE," *J. Jilin Univ. (Eng. Technol. Ed.)*, vol. 38, no. 5, pp. 1015–1019, Sep. 2008.
[49] K. Qin, M. Li, J. Guo, Y. Ai, and J. Gao, "On-road test and evaluation of emissions and fuel economy of the hybrid electric bus," SAE Tech. Paper 2009-01-1866, Jan. 2009, doi: 10.4271/2009-01-1866.
[50] B. H. Wang, Y. G. Luo, and J. W. Zhang, "simulation of city bus performance based on actual urban driving cycle in China," *Int. J. Automotive Technol.*, vol. 9, pp. 501–507, Aug. 2008.

[51] G. Fontaras, P. Pistikopoulos, and Z. Samaras, "Experimental evaluation of hybrid vehicle fuel economy and pollutant emissions over real-world simulation driving cycles," *Atmos. Environ.*, vol. 42, no. 18, pp. 4023–4035, 2008.
[52] G. Zamboni, M. André, M. Capobianco, and A. Roveda, "Experimental evaluation of heavy duty vehicle speed patterns in urban and port areas and estimation of their fuel consumption and exhaust emissions," *Transp. Res. D, Transp. Environ.*, vol. 35, pp. 1–10, Mar. 2015.
[53] D. Shi, L. Chu, J. Guo, Z. Wang, and R. Liu, "Energy control strategy of plug-in hybrid electric vehicle based on pattern recognition," *Adv. Mech. Eng.*, vol. 9, pp. 1–18, Mar. 2017.

DAPAI SHI was born in 1989. He received the B.S. degree in automobile service engineering from HuangHuai University, Zhumadian, China, in 2012, and the M.S degree in vehicle engineering from the Shandong University of Technology, Zibo, China, in 2015, respectively. He is currently pursuing the Ph.D. degree in vehicle engineering with Jilin University, Changchun, China.

He has authored four journals. In 2014, he published an article entitled Real-time Control Strategy of Elman Neural Network for the Parallel Hybrid Electric Vehicle in the *Journal of Applied Mathematics*. In 2017, he published an article entitled Energy Control Strategy of PHEV Based on Pattern Recognition in the *Advances in Mechanical Engineering*. Besides, he has taken part in projects, which are Jilin Science and Technology Development Plan Project (20170204085GX), the 863 national high technology research and development program of China (2012AA110903), and Jilin industrial technology innovation strategic alliance project (20150309013GX). His research interests include control systems engineering and energy, intelligent systems engineering, and theory and optimal energy control strategy about hybrid electric vehicles.

LIANG CHU (M'08) was born in 1967. He received the B.S., M.S., and Ph.D. degrees in vehicle engineering from Jilin University, Changchun, China. He is currently a Professor and the Doctoral Supervisor with the College of Automotive Engineering, Jilin University. His research interests include the driving and braking theory and control technology for hybrid electric vehicles, which conclude powertrain and brake energy recovery control theory and technology on electric vehicles and hybrid vehicles, theory and technology of hydraulic antilock braking and stability control for passenger cars, and the theory and technology of air brake ABS, and the stability control for commercial vehicle.

Dr. Chu has been a SAE Member. He was a member at the Teaching Committee of Mechatronics Discipline Committee of China Machinery Industry Education Association in 2006.

JIANHUA GUO was born in 1976. He received the Ph.D. degree in vehicle engineering, with a major in power machinery and Engineering (internal combustion engine), from Jilin University, Changchun, China. He is currently an Associate Professor with the College of Automotive Engineering of Jilin University. His main research interests include new energy vehicles, including hybrid electric vehicles, pure electric vehicles, control strategies, parameter matching, and powertrain control.

Since his graduation, he has participated in 14 projects at the National, Provincial, and Ministerial level and a total of over 30 papers published. Among them, 25 papers were retrieved by EI and ten by the first author. Besides, he has five patents for invention. He edited or enrolled in a series of five books. Among them, the editor's books included *Mechanical Parts* and *Practical automotive English*.

GUANGDONG TIAN received the B.S. degree in vehicle engineering from the Shandong University of Technology, Zibo, China, in 2007, and the M.S. and Ph.D. degrees in automobile application engineering from Jilin University, Changchun, China, in 2009 and 2012, respectively.

He is currently an Associate Professor with the Transportation College, Jilin University, China, and a Founding Member of Sustainable Production and Service Automation in the IEEE Robotics and Automation Society. He is invited to organize several conferences and service a Session Chair, including ICAMechS 2015 and CASE 2016. His research interests include remanufacturing and green manufacturing, green logistics and transportation, the intelligent inspection and repair of automotive, decision making, and intelligent optimization. He has authored over 70 journal and conference proceedings papers in the above research areas, including the IEEE TRANSACTIONS ON AUTOMATION SCIENCE ENGINEERING, the IEEE TRANSACTIONS ON CYBERNETICS, and the IEEE/ACM TRANSACTIONS ON COMPUTATIONAL BIOLOGY. In addition, he serves as a Frequent Reviewer for over 20 international journals, including the IEEE TRANSACTIONS ON AUTOMATION SCIENCE ENGINEERING, the IEEE TRANSACTIONS ON SYSTEMS, MAN, AND CYBERNETICS—Part A, and the *Asian Jouranl of Control*. He is listed in Marquis Who's Who in the World, 30th Edition, 2013.

YIXIONG FENG received the B.S. and M.S. degrees in mechanical engineering from Yanshan University, Qinhuangdao, China, in 1997 and 2000, respectively, and the Ph.D. degree in mechanical engineering from Zhejiang University, Hangzhou, China, in 2004.

He is currently a Professor with the Department of Mechanical Engineering, Zhejiang University, China, where he is also a member of the State Key Laboratory of Fluid Power Transmission and Control. He has been in charge of four different projects supported by the National Natural Science Foundation of China and one project supported by National High-tech Research and Development Program of China (863 Program). His research interests include mechanical product design theory, intelligent automation, and advance manufacture technology. He has authored over 100 journal and conference proceedings papers in the above research areas. He is received Zhejiang Province Outstanding Youth Fund and the National Outstanding Youth Fund.

ZHIWU LI (M'06–SM'07–F'16) received the B.S. degree in mechanical engineering, the M.S. degree in automatic control, and the Ph.D. degree in manufacturing engineering from Xidian University, Xi'an, China, in 1989, 1992, and 1995, respectively. He joined Xidian University in 1992. Over the past decade, he was a Visiting Professor with the University of Toronto, Technion (Israel Institute of Technology), Martin-Luther University, Conservatoire National des Arts et Métiers (Cnam), Meliksah Universitesi, King Saud University, and the University of Cagliari. He is currently with the Institute of Systems Engineering, Macau University of Science and Technology, Taipa, Macau. His current research interests include Petri net theory and application, the supervisory control of discrete event systems, work flow modeling and analysis, system reconguration, game theory, and data and process mining.

Dr. Li is a member of Discrete Event Systems Technical Committee of the IEEE Systems, Man, and Cybernetics Society, and a member of the IFAC Technical Committee on Discrete Event and Hybrid Systems from 2011 to 2014. He was a recipient of an Alexander von Humboldt Research Grant, Alexander von Humboldt Foundation, Germany, and Research in Paris, France. He is the Founding Chair of Xi'an Chapter of the IEEE Systems, Man, and Cybernetics Society. He serves as a Frequent Reviewer for over 60 international journals, including the *Automatica* and a number of the IEEE Transactions and many international conferences. He is listed in Marquis Who's Who in the world, 27th Edition, 2010.